

FINITE ELEMENT FLUX-CORRECTED TRANSPORT (FEM–FCT) FOR THE EULER AND NAVIER–STOKES EQUATIONS

RAINALD LÖHNER

*Berkeley Research Associates, Springfield, VA 22150, U.S.A. and Laboratory for Computational Physics and Fluid Dynamics,
Naval Research Laboratory, Washington, D. C. 20375, U.S.A.*

AND

KEN MORGAN, JAIME PERAIRE AND MEHDI VAHDATI

Institute for Numerical Methods in Engineering, University of Wales, Swansea SA2 8PP, Wales, U.K.

SUMMARY

A high resolution finite element method for the solution of problems involving high speed compressible flows is presented. The method uses the concepts of flux-corrected transport and is presented in a form which is suitable for implementation on completely unstructured triangular or tetrahedral meshes. Transient and steady-state examples are solved to illustrate the performance of the algorithm.

INTRODUCTION

Over the past few years, there has been an ongoing interest in the application of unstructured grid finite element methods to the solution of problems of high-speed compressible flow. In this area, the authors^{1–3} have proposed a two-step explicit implementation of a second order Taylor–Galerkin procedure^{4,5} and have used this approach to solve successfully a variety of inviscid and viscous problems. The addition of artificial viscosity is required to stabilize this solution procedure when it is applied to the analysis of problems involving strong discontinuities, and this has the effect of spreading flow discontinuities over several computational cells.

Solution methods based upon high resolution schemes^{6–11} give sharper definition of flow discontinuities, and are supposedly more robust. In two and three dimensions, these methods are generally implemented by using operator splitting and applying one-dimensional concepts in each co-ordinate direction separately. The finite element practitioner, however, finds difficulty in operating in this same manner, as the use of unstructured grids makes this approach impractical. The one high resolution method which can be used directly on unstructured grids in Zalesak's¹² multidimensional generalization of the one-dimensional flux-corrected transport (FCT) ideas of Boris and Book.^{13–15} This method employs a high-order scheme together with a low-order scheme and attempts to combine these in such a way that the high-order solution is used in smooth regions

Based on a contributed paper.

of the flow, whereas the low-order solution is favoured near discontinuities. The low-order scheme should produce monotonic results for the problem to be solved. Erlebacher¹⁶ and Parrott and Christie¹⁷ showed how FCT ideas could be interpreted in the finite element context for a single governing equation and implemented on triangular meshes. Our contribution is the extension of the technique to deal with the solution of a system of equations and the formulation of a scheme with high temporal accuracy, which is well-suited for the analysis of transient problems. The numerical examples presented to demonstrate the performance of the algorithm involve the solution of both steady and transient flows of inviscid and viscous fluids.

THE EQUATIONS OF COMPRESSIBLE FLOW

The governing equations of compressible flow can be written in the conservation form

$$\frac{\partial U}{\partial t} + \frac{\partial F_j^a}{\partial x_j} = \frac{\partial F_j^v}{\partial x_j}, \quad (1)$$

where the summation convention has been employed and

$$U = \begin{Bmatrix} \rho \\ \rho u_i \\ \rho e \end{Bmatrix}, \quad F_j^a = \begin{Bmatrix} \rho u_j \\ \rho u_i u_j + p \delta_{ij} \\ u_j (\rho e + p) \end{Bmatrix}, \quad F_j^v = \begin{Bmatrix} 0 \\ \sigma_{ij} \\ u_i \sigma_{ij} + k \frac{\partial T}{\partial x_j} \end{Bmatrix}. \quad (2)$$

Here ρ, p, e, T and k denote the density, pressure, specific total energy, temperature and thermal conductivity of the fluid, respectively, and u_i is the component of the fluid velocity in the direction x_i of a Cartesian co-ordinate system. The equation set is completed by the addition of the state equations

$$p = (\gamma - 1)\rho[e - \frac{1}{2}u_j u_j], \quad T = [e - \frac{1}{2}u_j u_j]c_v \quad (3)$$

which are valid for perfect gas, where γ is the ratio of the specific heats and c_v is the specific heat at constant volume. The components of the viscous stress tensor σ_{ij} are given by

$$\sigma_{ij} = \mu \left(\frac{\partial u_i}{\partial x_j} + \frac{\partial u_j}{\partial x_i} \right) + \lambda \frac{\partial u_k}{\partial x_k} \delta_{ij} \quad (4)$$

and it is assumed that λ and μ are related by

$$\lambda = -\frac{2\mu}{3}. \quad (5)$$

THE FLOW SOLVER: FEM-FCT

As stated above, high resolution, monotonicity preserving schemes must be developed in order to be able to simulate the strong non-linear discontinuities present in the flows under consideration. Although the pertinent literature abounds with high resolution schemes,⁶⁻¹¹ only Zalesak's generalization¹² of the one-dimensional FCT schemes of Boris and Book¹³⁻¹⁵ can be considered a truly multidimensional high resolution scheme. We remark here that the use of unstructured grids requires such truly multidimensional schemes, as the lack of lines or planes in the mesh inhibits the use of operator splitting.

Erlebacher¹⁶ and Parrot and Christie¹⁷ first analysed FCT schemes in the context of finite

element methods. We develop their ideas further to include the consistent mass, which yields high temporal accuracy, and to systems of equations.

The concept of flux-corrected transport (FCT)

We consider a set of conservation laws given by a system of partial differential equations of the form given equation (1), and assume that the advective fluxes $F^a = F^a(U)$ play a dominant role over the viscous fluxes $F^v = F^v(U)$. For flows described by equation (1), discontinuities in the variables may arise (e.g. shocks or contact discontinuities). Any numerical scheme of order higher than one will produce overshoots or ripples at such discontinuities (the so-called ‘Godunov theorem’¹⁸). Very often, particularly for mildly non-linear systems, these overshoots can be tolerated. However, for the class of problems studied here, overshoots will eventually lead to numerical instability, and will therefore have to be suppressed.

The idea behind FCT is to combine a high-order scheme with a low-order scheme in such a way that in regions where the variables under consideration vary smoothly (so that a Taylor expansion makes sense) the high-order scheme is employed, whereas in those regions where the variables vary abruptly the schemes are combined, in a conservative manner, in an attempt to ensure a monotonic solution.

The temporal discretization of equation (1) yields

$$U^{n+1} = U^n + \Delta U, \quad (6)$$

where ΔU is the increment of the unknowns obtained for a given scheme at time $t = t^n$. Our aim is to obtain a ΔU of as high an order as possible without introducing overshoots. To this end, we rewrite equation (6) as

$$U^{n+1} = U^n + \Delta U^1 + (\Delta U^h - \Delta U^1), \quad (7)$$

$$U^{n+1} = U^1 + (\Delta U^h - \Delta U^1). \quad (8)$$

Here ΔU^h and ΔU^1 denote the increments obtained by some high- and low-order schemes, respectively, whereas U^1 is the monotone, ripple-free solution at time $t = t^{n+1}$ of the low-order scheme. The idea behind FCT is to limit the second term on the right-hand side of equation (8):

$$U^{n+1} = U^1 + \lim (\Delta U^h - \Delta U^1), \quad (9)$$

in such a way that no new over/undershoots are created.

It is at this point that a further constraint, given by the conservation law (1) itself must be taken into account: strict conservation on the discrete level should be maintained. The simplest way to guarantee this for node-centred schemes (and we will only consider those here) is by constructing schemes for which the sum of the contributions of each individual element (cell) to its surrounding nodes vanishes (‘all that comes in goes out’). This means that the limiting process equation (9) will have to be carried out in the elements (cells).

Algorithmic implementation

We can now define FCT in a quantitative way. We follow Zalesak’s exposition,¹² but modify the term ‘flux’ by ‘element contribution to a node’. Those more familiar with finite volume or finite difference schemes should replace ‘element’ by ‘cell’ in what follows.

FCT consists of the following six algorithmic steps:

1. Compute LEC: the ‘low-order element contribution’ from some low-order scheme guaranteed to give monotonic results for the problem at hand.
2. Compute HEC: the ‘High-order element contribution’, given by some high-order scheme.
3. Define AEC: the ‘antidiffusive element contributions’:

$$\text{AEC} = \text{HEC} - \text{LEC}.$$

4. Compute the updated low-order solution:

$$U^1 = U^n + \sum_{el} \text{LEC} = U^n + \Delta U^1 \tag{10}$$

5. Limit or ‘correct’ the AEC so that U^{n+1} as computed in step 6 below is free of extrema not also found in U^1 or U^n :

$$\text{AEC}^c = \text{Cel} * \text{AEC}, 0 \leq \text{Cel} \leq 1. \tag{11}$$

6. Apply the limited AEC:

$$U^{n+1} = U^1 + \sum_{el} \text{AEC}^c. \tag{12}$$

The limiting procedure

Obviously, the whole approach depends critically on the all-important step 5 above. We define the following quantities:

- (a) P_I^\pm : the sum of all positive (negative) antidiffusive element contributions to node I :

$$P_I^\pm = \sum_{el} \left\{ \begin{matrix} \max \\ \min \end{matrix} \right\} (0, \text{AEC}_{el})$$

- (b) Q_I^\pm : the maximum (minimum) increment (decrement) node I is allowed to achieve in step 6 above:

$$Q_I^\pm = U_I^{\max/\min} - U^1,$$

where $U_I^{\max/\min}$ (defined below) represents the maximum (minimum) value the unknown U at node I is allowed to achieve in step 6 above

- (c) R^\pm :

$$R^\pm := \begin{cases} \min(1, Q^\pm/P^\pm), & \text{if } P^+ > 0, \quad P^- < 0, \\ 0, & \text{if } P^\pm = 0. \end{cases}$$

Now take, for each element:

$$\text{Cel} = \min(\text{element nodes}) \begin{cases} R^+, & \text{if } \text{AEC} > 0, \\ R^-, & \text{if } \text{AEC} < 0. \end{cases} \tag{13}$$

Finally, we obtain $U_I^{\max/\min}$ in three steps:

- (a) maximum (minimum) nodal U of U^n and U^1 :

$$U_I^* = \left\{ \begin{matrix} \max \\ \min \end{matrix} \right\} (U_I^1, U_I^n)$$

- (b) maximum (minimum) nodal value of element:

$$U_{el}^* = \begin{cases} \max \\ \min \end{cases} \{U_A^*, U_B^*, \dots, U_C^*\},$$

where A, B, \dots, C represent the nodes of element el

(c) maximum (minimum) U of all elements surrounding node I :

$$U_I^{\max} = \begin{cases} \max \\ \min \end{cases} \{U_1^*, U_2^*, \dots, U_m^*\},$$

where $1, 2, \dots, m$ represent the elements surrounding node I .

This completes the description of the limiting procedure. Up to this point we have been completely general in our description, so that equations (6)–(13) may be applied to any FEM–FCT scheme. In what follows, we restrict the exposition to the finite element schemes employed in the present work, describing the high and low-order schemes used.

The high-order scheme: consistent-mass Taylor–Galerkin

As the high-order scheme, we employ a two-step form^{1–3} of the one-step Taylor–Galerkin schemes described in References 4 and 5. These schemes belong to the Lax–Wendroff class, and could be substituted by any other high-order scheme which appears more convenient, including implicit schemes. Given the system of equations (1), we advance the solution from t^n to $t^{n+1} = t^n + \Delta t$ as follows:

(a) *First step (advective predictor).*

$$U^{n+1/2} = U^n - \frac{\Delta t}{2} \frac{\partial F_j^a}{\partial x_j} \Big|_n. \quad (14)$$

(b) *Second step.*

$$\Delta U^n = U^{n+1} - U^n = -\Delta t \frac{\partial F_j^a}{\partial x_j} \Big|_n^{n+1/2} + \Delta t \frac{\partial F_j^v}{\partial x_j} \Big|_n. \quad (15)$$

The spatial discretization of (14) and (15) is performed via the classic Galerkin weighted residual method,^{1–3} using linear elements, i.e. three-noded triangles in two dimensions and four-noded tetrahedra in three dimensions. For (15) the following system of equations is obtained:

$$M_C \Delta U^n = R^n, \quad (16)$$

where M_C denotes the consistent mass matrix,^{1–3} ΔU the vector of nodal increments and R the vector of added element contributions to the nodes. As M_C possesses an excellent condition number, equation (16) is never solved directly, but iteratively, requiring typically three passes⁵. We recast the converged solution of equation (16) into the following form, which will be of use later on:

$$M_L \Delta U^h = R + (M_L - M_C) \Delta U^h. \quad (17)$$

Here M_L denotes the diagonal, lumped mass-matrix.⁵

The low-order scheme: lumped-mass Taylor–Galerkin plus diffusion

The requirement placed on the low-order scheme in any FCT-method is monotonicity. The low-

order scheme must not produce any artificial, or numerical, ‘ripples’ or ‘wiggles’. It is clear that the better the low-order scheme, the easier the resulting task of limiting will be. Therefore an obvious candidate for the low-order scheme is Godunov’s method.¹⁸ However, this scheme would be relatively expensive, and its extension to unstructured grids remains unclear.

We have so far added ‘mass-diffusion’ to the lumped-mass Taylor–Galerkin scheme in the context of FEM–FCT.^{19,20} This simplest and least expensive form of diffusion is obtained by subtracting the lumped mass-matrix from the consistent mass-matrix for linear elements:

$$\text{DIFF} = c_d(M_C - M_L)U^n. \quad (18)$$

The element matrix thus obtained for two-dimensional triangles is of the form

$$c_d(M_C - M_L)_{el} = -\frac{c_d \text{Vol}_{el}}{12} \begin{Bmatrix} 2 & -1 & -1 \\ -1 & 2 & -1 \\ -1 & -1 & 2 \end{Bmatrix}. \quad (19)$$

Observe that we cannot simply add this diffusion to the high-order scheme in order to obtain monotonic results, as a multipoint-coupling of the right-hand side occurs due to the consistent mass-matrix employed in the high-order scheme. The imposition of monotonicity can nevertheless be achieved by using a lumped mass-matrix instead. As the terms originating from the discretization of the fluxes F^i in (1) are the same as in (15), the low-order scheme is given by

$$M_L \Delta U^1 = R + \text{DIFF}. \quad (20)$$

Resulting antidiffusive element contributions

Subtracting (20) from (17) yields the equation

$$M_L(\Delta U^h - \Delta U^1) = R + (M_L - M_C)\Delta U^h - R - \text{DIFF}, \quad (21)$$

or, using equation (18),

$$\Delta U^h - \Delta U^1 = M_L^{-1}(M_L - M_C)(c_d U^n + \Delta U^h). \quad (22)$$

Note that all terms arising from the discretization of the fluxes F^i in (1), (15), (20) have now disappeared. This is of particular importance if the antidiffusive element contributions must be recomputed (small core memory machines), and real gas effects are taken into account (table look-up times are considerable) or real viscosity effects have to be included (Navier–Stokes equations).

Limiting for systems of equations

The results available in the literature^{13–15} and our own experience^{19,20} have shown that, with FCT, results of excellent quality can be obtained for a single PDE. However, when trying to extend the limiting process to systems of PDEs, no immediately obvious or natural limiting procedure becomes apparent. Obviously, for one-dimensional problems one could advect each simple wave system separately, and then assemble the solution at the new time step. However, for multidimensional problems such a splitting is not possible, as the acoustic waves are circular. FDM–FCT codes used for production runs^{21,22} have so far limited each equation separately, invoking operator-splitting arguments. This approach does not always give very good results, as may be seen from Sod’s comparison of schemes for the Riemann problem,²³ and has been a point of continuing criticism by those who prefer to use the more costly Riemann-solver-based, essentially one-dimensional, TVD schemes.^{6–11} It would therefore appear as attractive to introduce ‘system

character' for the limiter by combining the limiters for all equations of the system. Many variations are possible and can be implemented, giving different performance for different problems. We just list some of the possibilities here, commenting on them where empirical experience is available.

- (a) Independent treatment of each equation as in operator-split FCT: this is the least diffusive method, tending to produce an excessive amount of ripples in the non-conserved quantities (and ultimately also in the conserved quantities).
- (b) Use of the same limiter (C_{el}) for all equations: this produces much better results, seemingly because the phase errors for all equations are 'synchronized'. This was also observed by Harten and Zwaas²⁴ and Zhmakin and Fursenko²⁵ for a class of schemes very similar to FCT. We mention the following possibilities:
 - (i) use of a certain variable as 'indicator variable' (e.g. density, pressure, entropy)
 - (ii) use of the minimum of the limiters obtained for the density and the energy ($C_{el} = \min(C_{el}(\text{density}), C_{el}(\text{energy}))$): this produces acceptable results, although some undershoots for very strong shocks are present. This option is currently our preferred choice for transient problems.
 - (iii) use of the minimum of the limiters obtained for the density and the pressure ($C_{el} = \min(C_{el}(\text{density}), C_{el}(\text{pressure}))$): this again produces acceptable results, particularly for steady-state problems.

NUMERICAL EXAMPLES

Shock over an indentation

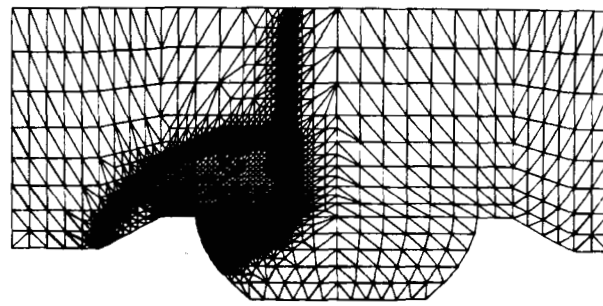
The first problem considered simulates the transient flow field produced by the interaction of a strong shock with an indentation in the ground. For this case, the shock Mach number was set to $M_s = 25$, which corresponds to a pressure-jump ratio of about 1:100. During the transient, pressure ratios as high as 1:1000 result. The problem statement, solution domain, spatial discretization and solutions obtained are shown in Figures 1(a)–(e). Note that an adaptive refinement scheme for transient problems²⁶ was used to reduce the overall storage and CPU requirements.

As the shock travels over the indentation, it produces a bow shock and a rarefaction (Figures 1(a), (b)). Then, it collides with the right wall of the indentation and bounces back, producing several shock/shock and shock/contact discontinuity interactions (Figures 1(c), (d)). Observe the level of physically relevant detail that the scheme is able to reproduce, e.g. the triple shock produced at $T = 0.12$ (Figures 1(d) (e)). The velocity pattern generated by these interactions has been magnified in Figure 1(e), and shows a large residual vortex, as well as the different shock fronts and other discontinuities. We remark that at all times the shocks are captured within 2 to 3 elements.

In the present case, we used as limiter for all equations the minimum of the limiters computed for the continuity and energy equations. It is found, that for the strong shocks present in such flow fields, even a pressure-undershoot of 0.1 per cent will lead to negative pressures. Therefore, the pressure is additionally limited artificially in order to be positive (albeit small) at all times.

Steady supersonic flow past a circular cylinder

This problem involves inviscid Mach 3 flow past a circular cylinder. The solution has been obtained by relaxing, with local time step, the transient solution towards the final steady state. During this iteration process, the grid was adapted three times to the solution by using an adaptive



NELEM=5897, NPOIN=3021

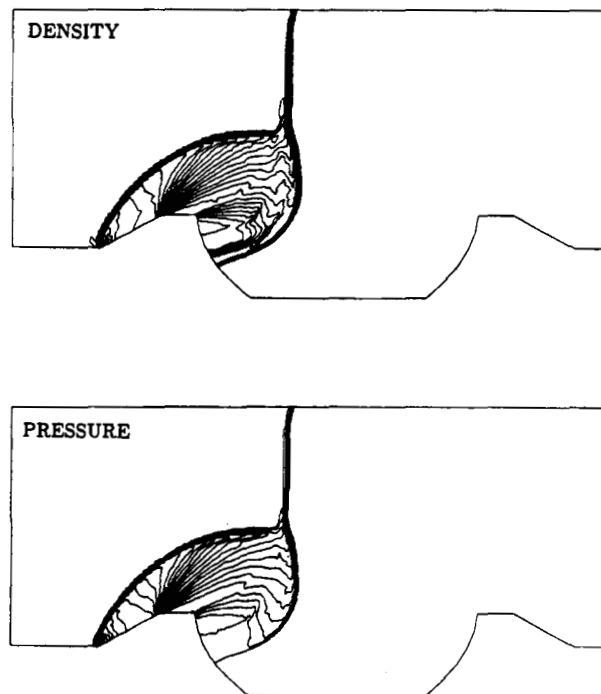
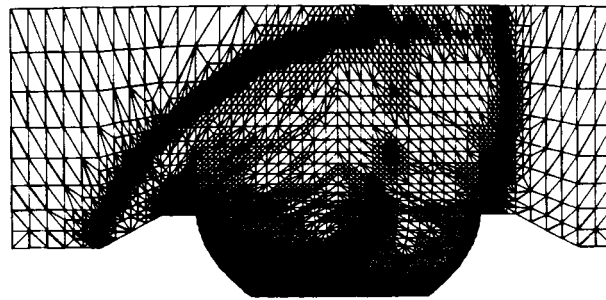


Figure 1(a). Shock over indentation: $T = 0.04$

mesh regeneration technique.²⁷ The final grid is shown in Figure 2(a). A detail of the pressure coefficient distribution is shown in Figure 2(b), and the variation of pressure coefficient along the centre line and over the cylinder surface is given in Figure 2(c).

Shock–bubble interaction

This problem is included here to demonstrate a new axisymmetric capability, and also to show that not only geometrically complex domains, but also physically complex problems can be handled economically by the methodologies developed. Initially, a weak shock ($M_s = 1.29$), coming from the left in Figure 3(a), travels into a bubble of heavier material. In the present case, the outer medium was assumed to be air, whereas the bubble was assumed to consist of freon. Owing to the



NELEM=11881, NPOIN=6073

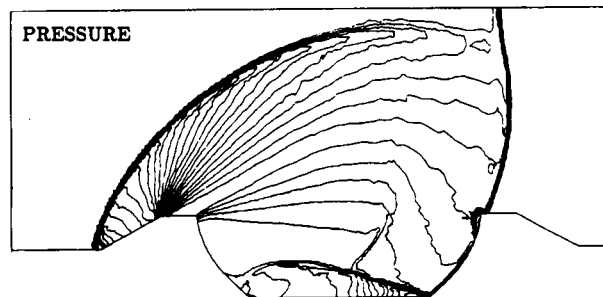
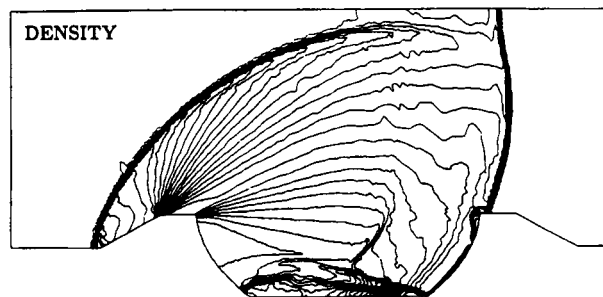
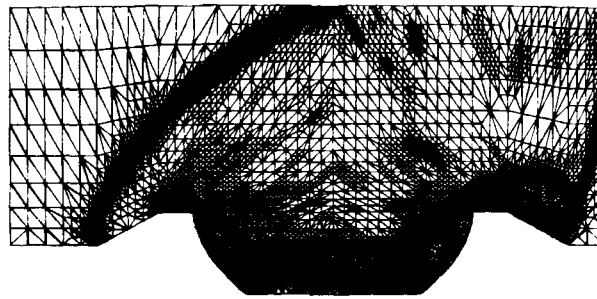


Figure 1(b). Shock over indentation: $T = 0.08$

higher density of freon, the shock speed inside the bubble decreases (Figure 3(b)). Whereas the outer shock bends over, the inner shock focuses at the right end of the bubble, producing a significant overpressure (Figure 3(c)), and initiating a small, circular blast wave (Figure 3(d)).

Steady supersonic flow over a flat plate

The fourth problem considered is the steady state solution of supersonic viscous flow over a flat plate. The flow conditions correspond identically to one of the cases considered by Carter,²⁸ using a finite difference scheme. The free stream Mach number is 3 and the Reynolds number based on the plate length is 1000. The temperature of the plate is assumed constant. The Sutherland viscosity law²⁹ is used and the initial conditions are chosen to be appropriate to the case of a flat plate



NELEM=13433, NPOIN=6862

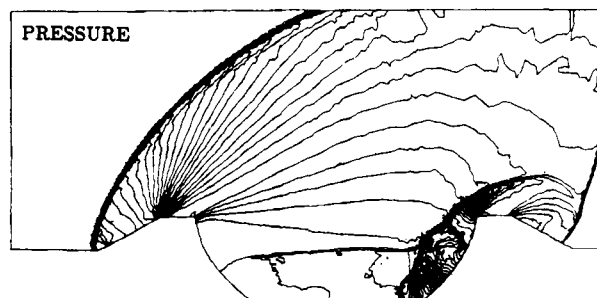
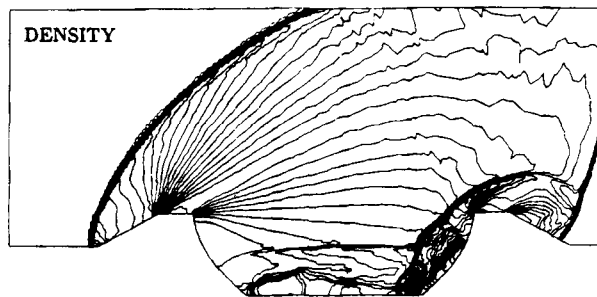
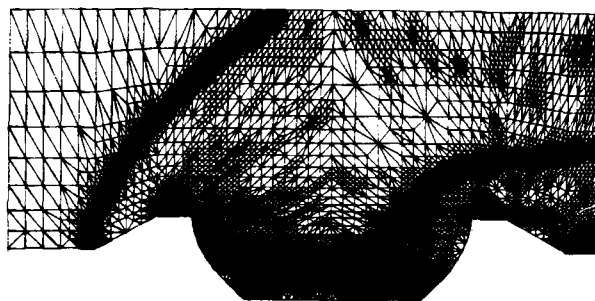


Figure 1(c). Shock over indentation: $T = 0.10$

impulsively inserted into the free stream. The mesh used is displayed in (Figure 4(a)), and the general features of the solution can be appreciated in the density contour plots shown in (Figure 4(b)). The variation of the computed wall pressure distribution is given in (Figure 4(c)).

CONCLUSIONS

It has been demonstrated how unstructured grids and high resolution schemes may be combined, yielding FEM-FCT. The numerical examples indicate that a high accuracy can be obtained economically for problems involving complex domains and/or adaptive mesh refinement. Furthermore, the 'equation-splitting' employed in classic FCT-codes^{21,22} has been extended by coupling or 'synchronizing' the limiters of all the equations involved, without taking recourse to more costly Riemann-solver-based monotone schemes.



NELEM=13852, NPOIN=7065

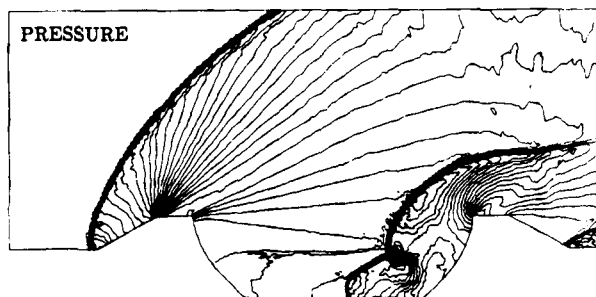
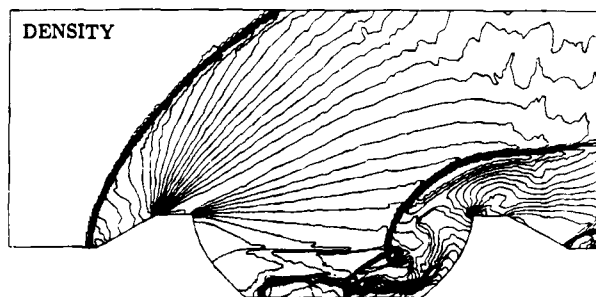


Figure 1(d). Shock over indentation: $T = 0.12$

Extensions of the present work are under investigation and involve the development of better limiters for systems of equations in the context of FEM-FCT, the extension of FEM-FCT to implicit or semi-implicit time-stepping schemes,³⁰ and the combination of FEM-FCT with unstructured multigrid methods³¹ for the rapid solution of steady-state problems.

ACKNOWLEDGEMENTS

It is a pleasure to acknowledge many fruitful and stimulating discussions during the course of the present work with Drs. J. P. Boris, D. L. Book and S. T. Zalesak.

This work was funded by the Office of Naval Research through the Naval Research Laboratory, and by the Aerothermal Loads Branch of the NASA Langley Research Center.

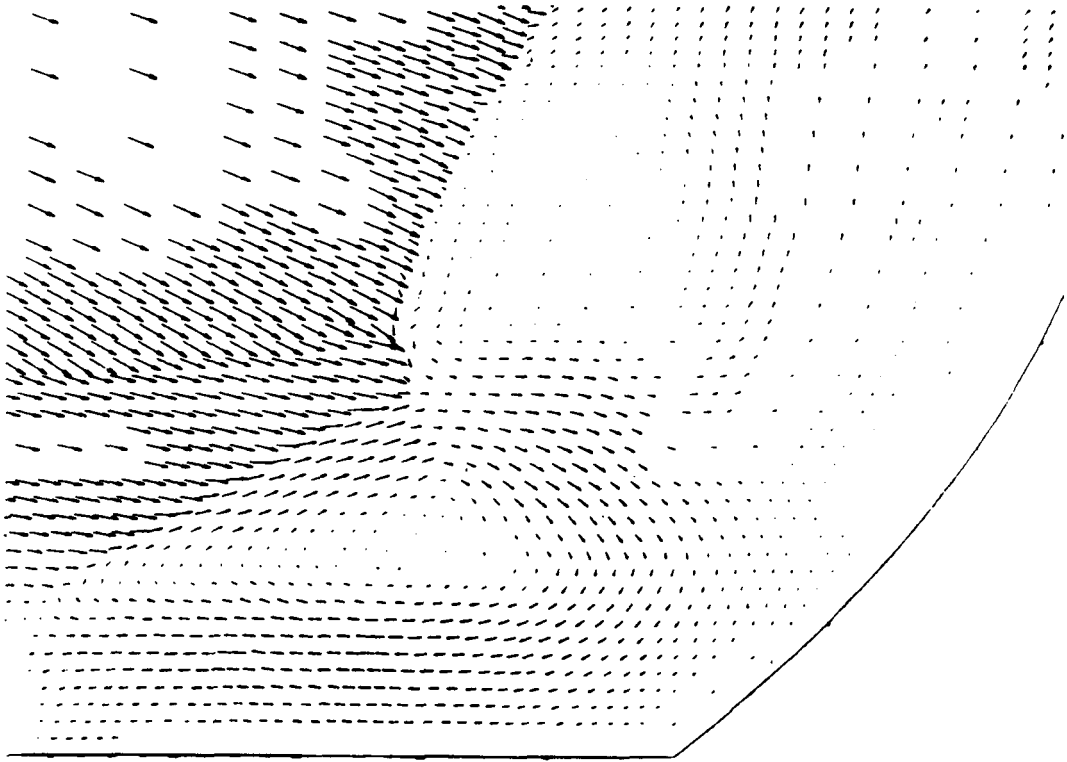


Figure 1(e). Velocity vectors at $T = 0.12$ (enlargement)

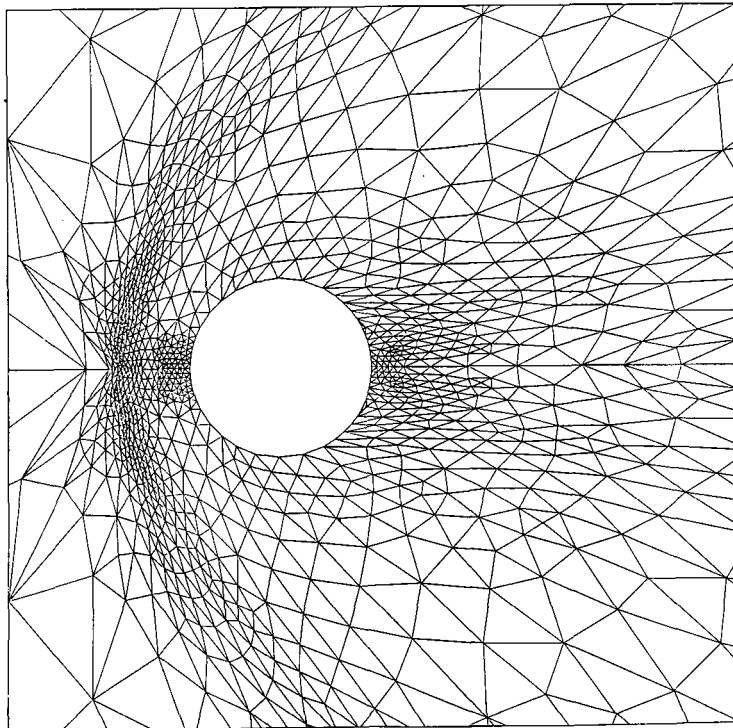


Figure 2(a). Steady supersonic flow past a cylinder: mesh

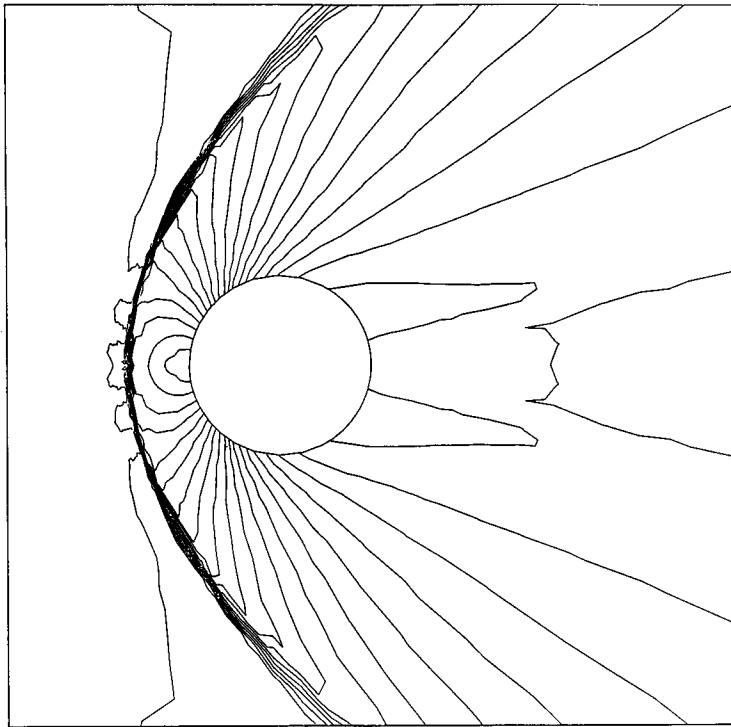


Figure 2(b). Steady supersonic flow past a cylinder: Pressure coefficient distribution

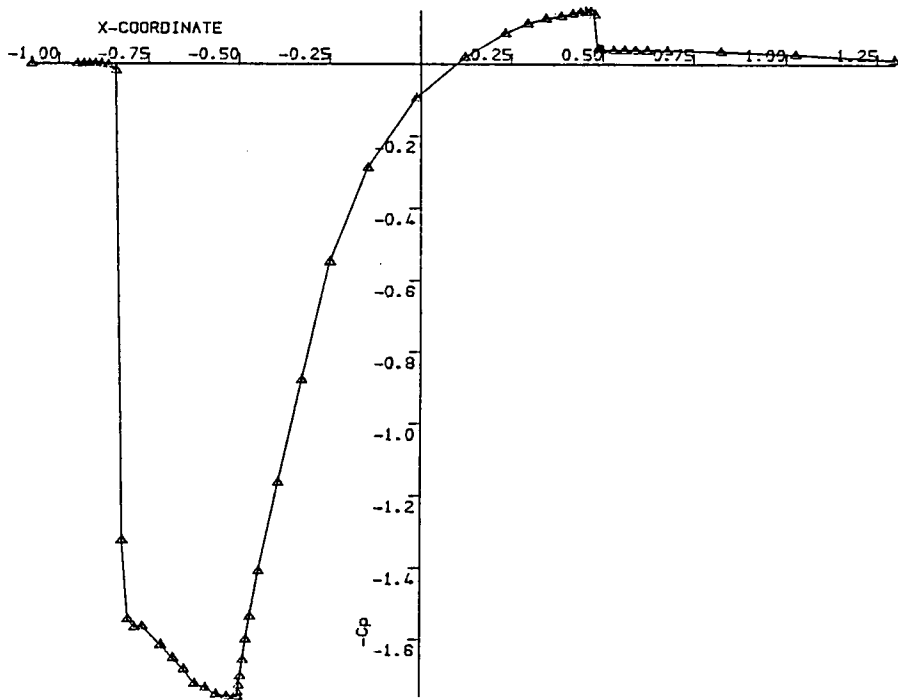
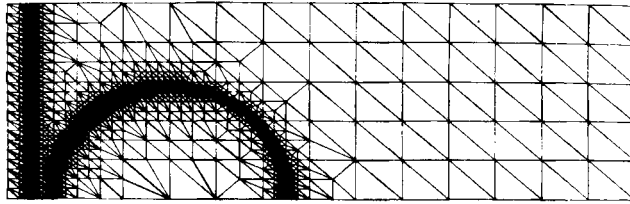


Figure 2(c). Steady supersonic flow past a cylinder: Variation of the pressure coefficient along the centre line and over the cylinder surface



NELEM=6635, NPOIN=3374

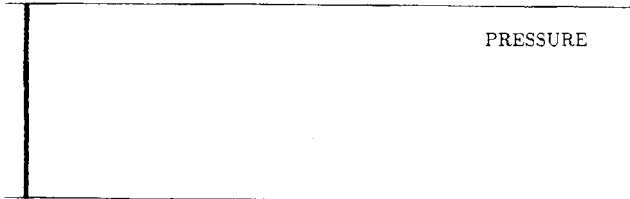
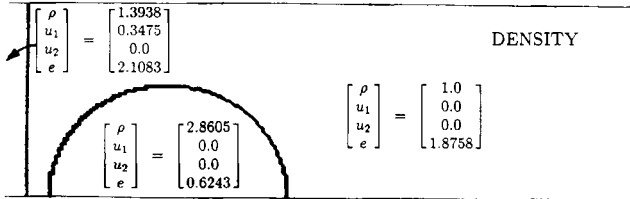
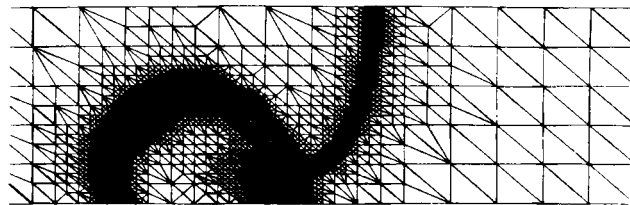


Figure 3(a). Shock-bubble interaction: $T = 0.0$



NELEM=14528, NPOIN=7335

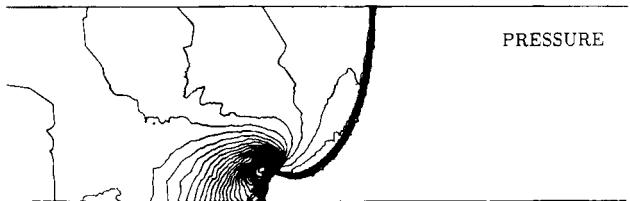
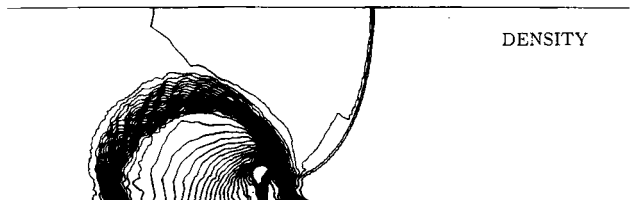
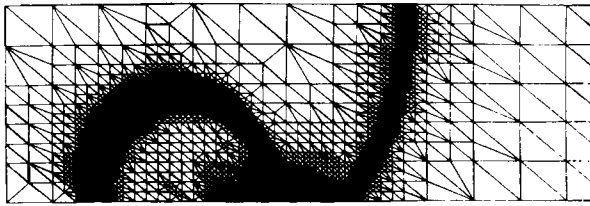


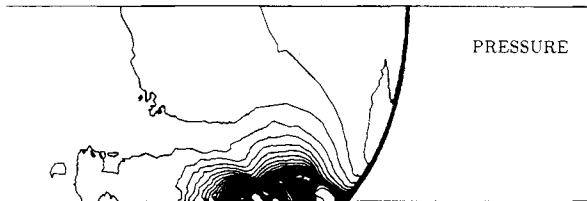
Figure 3(b). Shock-bubble interaction: $T = 0.6$



NELEM=16736, NPOIN=8464

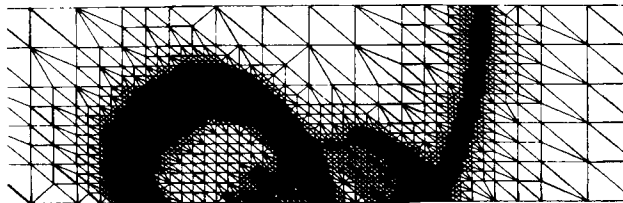


DENSITY



PRESSURE

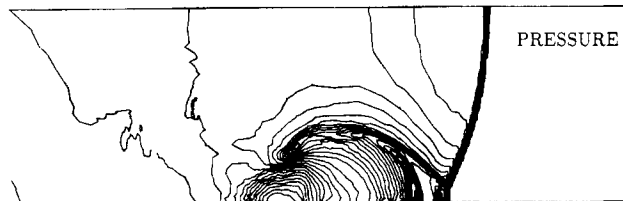
Figure 3(c). Shock-bubble interaction: $T = 0.7$



NELEM=16577, NPOIN=8386

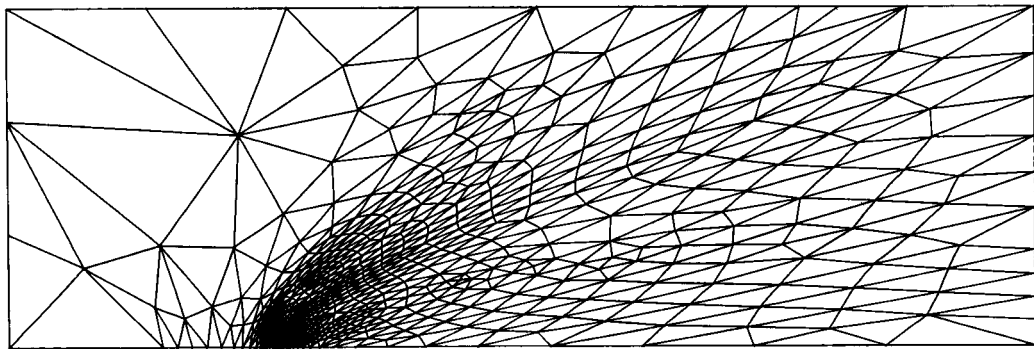


DENSITY

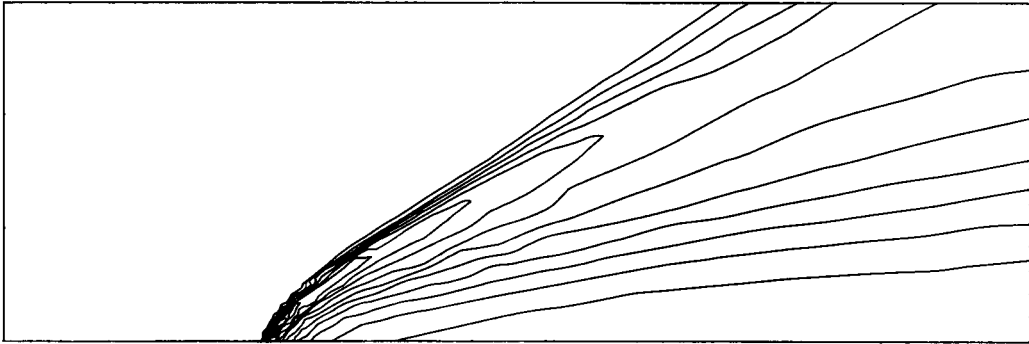


PRESSURE

Figure 3(d). Shock-bubble interaction: $T = 0.8$



(a)



(b)

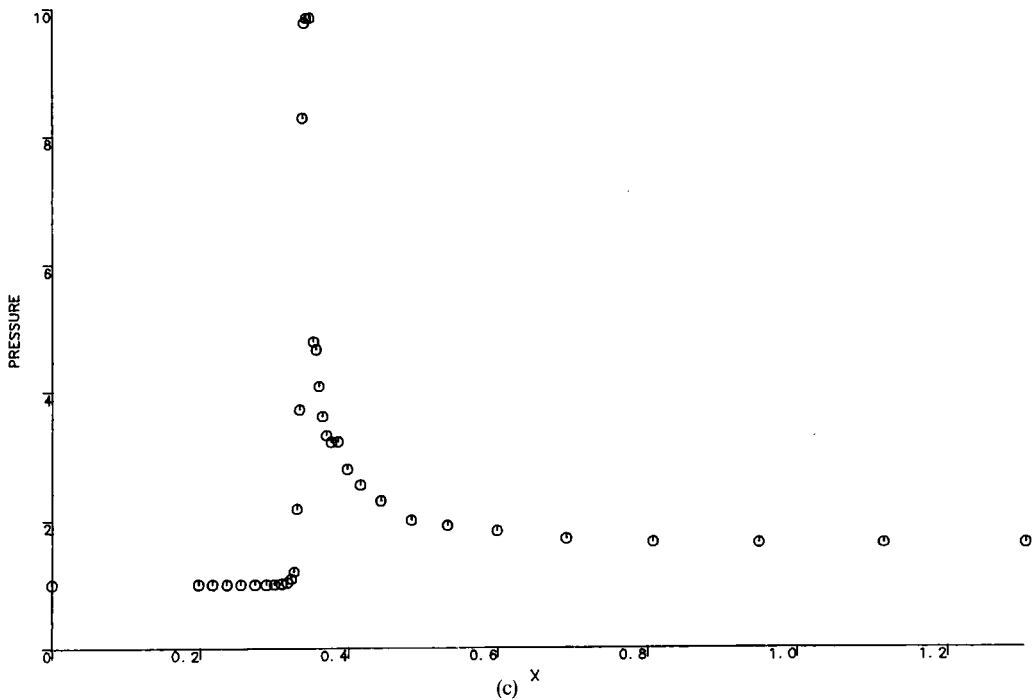


Figure 4. Mach 3 flow past a flat plate, Reynolds number. 1000: (a) mesh; (b) density contours; (c) pressure variation along the line of the plate

REFERENCES

1. R. Löhner, K. Morgan and O. C. Zienkiewicz, 'An adaptive finite element procedure for high speed flows', *Comp. Meth. Appl. Mech. Eng.*, **51**, 441–465 (1985).
2. R. Löhner, K. Morgan, J. Peraire and O. C. Zienkiewicz, 'Finite element methods for high speed flows', *AIAA-85-1531-CP*, 1985.
3. R. Löhner, K. Morgan, J. Peraire, O. C. Zienkiewicz and L. Kong, 'Finite element methods for compressible flow', in K. W. Morton and M. J. Baines (eds), *Numerical Methods for Fluid Dynamics*, Oxford University Press, 1986, pp. 28–53.
4. J. Donea, 'A Taylor–Galerkin method for convective transport problems', *Int. j. numer. methods Eng.*, **20**, 101–119 (1984).
5. R. Löhner, K. Morgan and O. C. Zienkiewicz, 'The solution of non-linear hyperbolic equation systems by the finite element method', *Int. j. numer. methods Fluids*, **4**, 1043–1063 (1984).
6. P. Woodward and P. Colella, 'The numerical simulation of two-dimensional fluid flow with strong shocks', *J. Comp. Phys.*, **54**, 115–173 (1984).
7. B. van Leer, 'Towards the ultimate conservative scheme. II. Monotonicity and conservation combined in a second order scheme', *J. Comp. Phys.*, **14**, 361–370 (1974).
8. P. L. Roe, 'Approximate Riemann solvers, parameter vectors and difference schemes', *J. Comp. Phys.*, **43**, 357–372 (1981).
9. S. Osher and F. Solomon, 'Upwind difference schemes for hyperbolic systems of conservation laws', *Math. Comp.*, **38**, 339–374 (1982).
10. A. Harten, 'High resolution schemes for hyperbolic conservation laws', *J. Comp. Phys.*, **49**, 357–393 (1983).
11. P. K. Sweby, 'High resolution schemes using flux limiters for hyperbolic conservation laws', *SIAM J. Num. Anal.*, **21**, 995–1011 (1984).
12. S. T. Zalesak, 'Fully multidimensional flux-corrected transport algorithm for fluids', *J. Comp. Phys.*, **31**, 335–362 (1979).
13. J. P. Boris and D. L. Book, 'Flux-corrected transport. I. SHASTA, a transport algorithm that works', *J. Comp. Phys.*, **11**, 38–69 (1973).
14. D. L. Book, J. P. Boris and K. Hain, 'Flux-corrected transport. II. Generalizations of the method', *J. Comp. Phys.*, **18**, 248–283 (1975).
15. J. P. Boris and D. L. Book, 'Flux-corrected transport. III. Minimal-error FCT algorithms', *J. Comp. Phys.*, **20**, 397–431 (1976).
16. G. Erlebacher, 'Solution adaptive triangular meshes with application to the simulation of plasma equilibrium', *Ph.D. Thesis*, Columbia University, 1984.
17. A. K. Parrott and M. A. Christie, 'FCT applied to the 2-D finite element solution of tracer transport by single phase flow in a porous medium', in K. W. Morton and M. J. Baines (eds), *Numerical Methods for Fluid Dynamics*, Oxford University Press, 1986, pp. 609–620.
18. S. K. Godunov, 'Finite difference method for numerical computation of discontinuous solutions of the equations of fluid dynamics', *Mat. Sb.*, **47**, 271–306 (1959).
19. R. Löhner, K. Morgan, M. Vahdati, J. P. Boris and D. L. Book, 'FEM-FCT: combining high resolution with unstructured grids', submitted to *J. Comp. Phys.* (1986).
20. K. Morgan, R. Löhner, J. R. Jones, J. Peraire and M. Vahdati, 'Finite element FCT for the Euler and Navier–Stokes Equations', *Proc. 6th Int. Symp. Finite Element Methods in Flow Problems*, INRIA, 1986.
21. M. A. Fry and D. L. Book, 'Adaptation of flux-corrected transport codes for modelling dusty flows', in R. D. Archer and B. E. Milton (eds), *Proc. 14th Int. Symp. on Shock Tubes and Waves*, New South Wales University Press, 1983.
22. D. E. Fyfe, J. H. Gardner, M. Picone and M. A. Fry, 'Fast three-dimensional flux-corrected transport code for highly resolved compressible flow calculations', *Springer Lecture Notes in Physics*, **218**, Springer Verlag, 1985, pp. 230–234.
23. G. Sod, 'A survey of several finite difference methods for systems of nonlinear hyperbolic conservation laws', *J. Comp. Phys.*, **27**, 1–31 (1978).
24. A. Harten and G. Zwaas, 'Self-Adjusting hybrid schemes for shock computations', *J. Comp. Phys.*, **6**, 568–583 (1972).
25. A. I. Zhmakin and A. A. Fursenko, 'A class of monotonic shock-capturing difference schemes', *NRL Memo. Rep. 4567*, 1981.
26. R. Löhner, 'An adaptive finite element scheme for transient problems in CFD', to appear in *Comp. Meth. Appl. Mech. Eng.* (1987).
27. J. Peraire, M. Vahdati, K. Morgan and O. C. Zienkiewicz 'Adaptive remeshing for compressible flow computations', to appear in *J. Comp. Phys.* (1987).
28. J. E. Carter, 'Numerical solutions of the Navier–Stokes equations for the supersonic laminar flow over a two-dimensional compression corner', *NASA Tech. Rep. R-385*, 1972.
29. H. Schlichting, *Boundary Layer Theory*, McGraw-Hill, 1979.
30. G. Patnaik, R. H. Guirguis, J. P. Boris and E. S. Oran, 'A barely implicit correction for flux-corrected transport', to appear in *J. Comp. Phys.* (1987).
31. R. Löhner and K. Morgan, 'An unstructured multigrid method for elliptic problems', *Int. j. numer. methods. eng.*, **24**, 101–115 (1987).